Check for updates

New Phytologist

Research

Wind acclimation in a subtropical forest: trees on wind-exposed slopes are shorter with smaller crowns

Roi Ankori-Karlinsky[1], Tobias D. Jackson[2], Gan Yuan[3], Jess K. Zimmerman[4], Douglas C. Morton[5], Tian Zheng[3] and María Uriarte[1]

[1]Department of Ecology, Evolution, and Environmental Biology, Columbia University, 1190 Amsterdam Avenue, New York, NY 10027, USA; [2]School of Biological Sciences, University of Bristol, Bristol, BS8 1TQ, UK; [3]Department of Statistics, Columbia University, 1255 Amsterdam Avenue, New York, NY 10027, USA; [4]Department of Environmental Sciences, University of Puerto Rico, San Juan, PR 00925, USA; [5]Biospheric Sciences Laboratory, NASA Goddard Space Flight Center, Greenbelt, MD 20771, USA

Author for correspondence:
Roi Ankori-Karlinsky
Email: roiak2@gmail.com

Received: *14 October 2024*
Accepted: *23 May 2025*

New Phytologist (2025)
doi: 10.1111/nph.70294

Key words: *Cecropia schreberiana*, *Dacryodes excelsa*, disturbance ecology, LiDAR, tree architecture, tree biomechanics, tropical forests, wind exposure.

Summary

- Tree architecture is an important component of forest community dynamics – taller trees with larger crowns often outcompete their neighbors, but they are generally at higher risk of wind-induced damage. Yet, we know little about wind impacts on tree architecture in natural forest settings, especially in complex tropical forests. Here, we use airborne light detection and ranging (LiDAR) and 30 yr of forest inventory data in Puerto Rico to ask whether and how chronic winds alter tree architecture.
- We randomly sampled 124 canopy individuals of four dominant tree species ($n = 22$–39). For each individual, we measured slenderness (height/stem diameter) and crown area (m^2) and evaluated whether exposure to chronic winds impacted architecture after accounting for topography (curvature, elevation, slope, and soil wetness) and neighborhood variables (crowding and previous hurricane damage). We then estimated the mechanical wind vulnerability of trees.
- Three of four species grew significantly shorter (2–4 m) and had smaller crown areas in sites exposed to chronic winds. A short-lived pioneer species, by contrast, showed no evidence of wind-induced changes.
- We found that three species' architectural acclimation to chronic winds resulted in reduced vulnerability. Our findings demonstrate that exposure to chronic, nonstorm winds can lead to architectural changes in tropical trees, reducing height and crown areas.

Introduction

Forest trees compete with each other in space to capture resources and recruitment opportunities (Loehle, 2000), while constrained by neighboring trees and the frequent threat of wind and other disturbances (Mitchell, 2013; MacFarlane & Kane, 2017). This balance of requirements can often be reflected in tree architecture (Malhi *et al.*, 2018) – taller trees with larger crowns are more photosynthetically efficient (Niklas & Kerchner, 1984), but they are also more exposed in the canopy, increasing their risk of breaking (Jackson *et al.*, 2019a). In forested areas frequently exposed to winds, trees may suffer branch loss from snapping or abrasion, or adjust their architecture through acclimation (i.e. growth changes) to reduce their wind risk.

Chronic wind exposure – frequent exposure to noncatastrophic winds (Momberg *et al.*, 2021) – can trigger differential growth responses in plants (Jaffe, 1973; Telewski, 1995). Experiments show that regular exposure to wind speeds, even as low as $\geq 8.3\ m\ s^{-1}$, can lead plants to invest in mechanical stability at the expense of height (Moulia & Combes, 2004), redirecting carbon allocation from height toward radial growth and root anchorage (Nicoll *et al.*, 2008; Bonnesoeur *et al.*, 2016). Trees exposed to chronic winds therefore may grow less slender (i.e. height to stem-width ratio) than those in more protected locations (Meguro & Miyawaki, 1994; Coomes *et al.*, 2018). Less slender trees and those with smaller crown areas are predicted to have lower vulnerability to damage from more severe wind disturbances (Cremer *et al.*, 1982; Jackson *et al.*, 2019a; Hall *et al.*, 2020). Therefore, chronic exposure to winds may lead to architectural changes that result in lower vulnerability to future wind-induced damage (Brüchert & Gardiner, 2006; Gardiner *et al.*, 2016; Jackson *et al.*, 2024). However, few studies have evaluated the effects of chronic winds on tree architecture in structurally complex natural forests.

Besides potential acclimation to chronic winds, the architecture of a tree is complex and depends on multiple factors – species' evolved life-history traits, stand disturbance history, crowding by neighboring trees, topography, and soil conditions (Peltola, 2006; MacFarlane & Kane, 2017; Moore *et al.*, 2018). For example, trees growing in crowded neighborhoods may have reduced growth due to resource competition (Fortunel *et al.*, 2018), growing shorter or smaller crowns as a result

© 2025 The Author(s).
New Phytologist © 2025 New Phytologist Foundation. This article has been contributed to by U.S. Government employees and their work is in the public domain in the USA.

14698137, 0, Downloaded from https://nph.onlinelibrary.wiley.com/doi/10.1111/nph.70294 by Maria Uriarte - Columbia University Libraries , Wiley Online Library on [12/06/2025]. See the Terms and Conditions (https://onlinelibrary.wiley.com/terms-and-conditions) on Wiley Online Library for rules of use; OA articles are governed by the applicable Creative Commons License

(MacFarlane & Kane, 2017). Topography also has pronounced impacts on tree growth: reduced root stability in water-saturated valleys or shallow soils on steep ridges can increase tree vulnerability to storm damage (Basnet, 1992; Basnet *et al.*, 1992), potentially leading to crown architecture changes for increased stability (Gardiner *et al.*, 2016). The disturbance history of a forest (e.g. when a severe windstorm most recently passed) may also lead to architectural changes due to changes in surrounding light conditions, which alter growth and therefore architecture (Jucker, 2022). Such site and stand conditions interact with life-history strategies related to light and water-use efficiency (Niklas, 1997; Loehle, 2000). For example, long-lived (i.e. centuries) shade-tolerant trees may prioritize mechanical stability over growth by allocating resources to grow deeper roots or denser stem wood that can reduce wind damage over long life spans (Basnet *et al.*, 1993; Gelder *et al.*, 2006; Rifai *et al.*, 2016). Short-lived (i.e. decades) pioneer species, meanwhile, may grow rapidly tall and risk wind damage over shorter lifetimes in exchange for increased growth and light capture (Uriarte *et al.*, 2004, 2012; Canham *et al.*, 2010; Flynn *et al.*, 2010).

Because of the complexity of these factors in understanding the architecture of trees in response to chronic winds, as well as the economic importance of plantation forests, most wind-tree studies have been conducted in more structurally uniform temperate or boreal forests (Anyomi *et al.*, 2016; Gardiner *et al.*, 2016). However, only a handful of studies have examined *tropical* forest trees' architecture and their response to winds (Gorgens *et al.*, 2021; Jackson *et al.*, 2021a; Jucker, 2022). The wind-tree studies that do exist in tropical forests mostly focus on severe disturbances such as hurricanes (Canham *et al.*, 2010; Uriarte *et al.*, 2019; Lin *et al.*, 2020), although chronic winds may have larger and more broadly distributed effects on tree structure and carbon dynamics (Ennos, 1997; Coomes *et al.*, 2018; Needham *et al.*, 2022). This scarcity of studies reflects the labor-intensive nature of quantifying tree architecture *in situ* (Lines *et al.*, 2022) and the difficulties of modeling the movement of winds over structurally complex forest canopies at the appropriate scales (Robertson, 1986; Boudreault *et al.*, 2015). Understanding the impacts of chronic winds on tropical trees under natural conditions is, therefore, an important knowledge gap, as structurally complex tropical forests are an essential part of the global carbon sink (Pan *et al.*, 2024). Fortunately, airborne laser scanning (ALS) technology now allows us to quantify crown height and shape of tall canopy trees even in structurally complex forests (LaRue *et al.*, 2020, 2023; Jucker, 2022). Moreover, some forests experience strong directionality of wind fields (Coomes *et al.*, 2018; Zimmerman *et al.*, 2021), allowing us to isolate the effects of chronic wind exposure on architecture and mechanical tree risk by comparing exposed and protected trees within the same forest environment.

Here, we ask whether chronic wind exposure leads to architectural changes in tropical trees, potentially affecting their estimated vulnerability to wind-induced stem breaks. To that aim, we calculated ALS-derived architectural metrics for 124 trees representing four common species and used their architecture to estimate their mechanical vulnerability to wind-induced damage. The species span a range of resource use and mechanical stability strategies in the Luquillo Experimental Forest (LEF) in Puerto Rico (Uriarte *et al.*, 2012, 2019). We then used 30 yr of forest inventory data, topographical information, and records of previous hurricane damage to assess the effects of chronic wind exposure on tree architecture and estimated wind vulnerability after accounting for multiple ancillary factors. Specifically, we hypothesized that chronically wind-exposed trees, in contrast to trees in sheltered areas, will:

H1: *Grow shorter and less slender.*

H2: *Will have smaller crown areas.*

H3: *These changes will lead to lower estimated mechanical vulnerability to severe winds.*

H4: *Longer-lived, more wood-dense species will show more pronounced wind-induced architectural changes.*

Materials and Methods

Study site

The Luquillo Forest Dynamics Plot (LFDP, 18°20′ N, 62°49′ W) is a 16-ha permanent forest plot in the LEF in El Yunque National Forest in northeast (NE) Puerto Rico (Thompson *et al.*, 2002). Mean annual rainfall is 3685 mm, elevation ranges from 332 to 427 m asl and slope from 3 to 60% (Thompson *et al.*, 2002). The topography includes northwest-running drainages that form NE- and southwest-facing slopes. Soils on the LFDP are clays formed from volcaniclastic sandstone that characteristically vary in soil type from well-drained uplands (Zarzal) to poorly drained side slopes and valleys (Johnston, 1992; Thompson *et al.*, 2002).

All tree stems in the LFDP ≥ 1 cm diameter at 1.3 m (diameter at breast height, dbh) have been identified, tagged, and mapped in censuses conducted approximately every 5 yr between 1990 and 2022 (Zimmerman *et al.*, 2021). The southern half of the plot is old-growth forest dominated by the late-successional species *Dacryodes excelsa* Vahl., *Manilkara bidentata* (A. DC.) Chev, and the palm *Prestoea acuminata* var *montana* (Thompson *et al.*, 2002). The early successional species *Cecropia schreberiana* Miq. is distributed in the LFDP and recruited in larger numbers after the passage of two hurricanes that made landfall in the LFDP – Hugo in 1989 and Georges in 1998, although Georges had minor effects in the LFDP (Canham *et al.*, 2010). By 2017, when airborne data for this study were collected, forest structure had largely recovered to pre-Hugo levels (Heartsill Scalley, 2017) – average basal area was 36.7 $m^2\,ha^{-1}$ at the time of hurricane Hugo, 30.85 $m^2\,ha^{-1}$ at the time Georges struck, and 38.37 $m^2\,ha^{-1}$ in 2016 (Uriarte *et al.*, 2019).

Chronic wind exposure

We calculated a topographically derived, canopy-independent model of chronic wind exposure. Variation in aspect leads to differential wind exposure in the LFDP (Fig. 1, Supporting

© 2025 The Author(s).
New Phytologist © 2025 New Phytologist Foundation. This article has been contributed to by U.S. Government employees and their work is in the public domain in the USA.

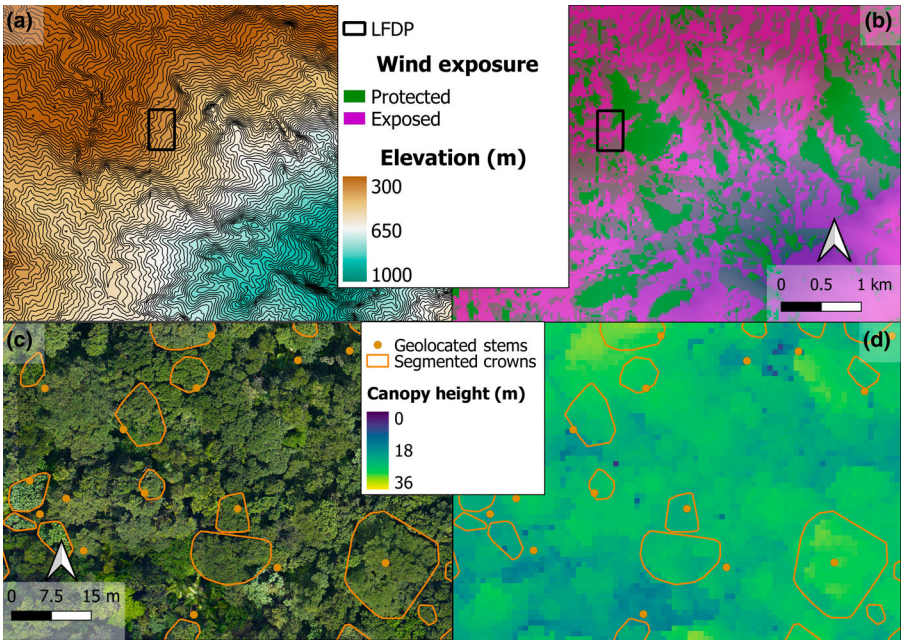

Fig. 1 Map of study sites in the Luquillo Forest Dynamics Plot (LFDP) – (a) Elevation (m), (b) Topographic exposure to chronic winds, (c) Geolocated tree stems with manually segmented crowns based on Goddard's LiDAR, Hyperspectral, and Thermal 0.03-m resolution RGB images, and (d) Airborne LiDAR (ALS) canopy height model. Note that (c, d) are a subset of the map in (a, b).

Information Fig. S1). To derive chronic wind directions, we extracted wind direction and speed data collected during 2002–2014 by a Met One 034A/B-L Wind Set (Campbell©, Logan, UT, USA) on the roof of the El Verde research station (*c.* 23 m aboveground, at 350 m asl) near the LFDP. Data were recorded daily on a 10× data logger (Campbell©) and downloaded every 2 wk (Ramirez, 2015). We removed outlier measurements of wind speeds ≥ 40 m s^{-1} and calculated the percentage of wind coming from 12, 30° sectors, considering prevailing wind direction as sectors accounting for > 10% of wind direction data. Only three sectors (30–60°, 60–90°, and 90–120°) met this criterion, accounting for 67% of wind direction observations and also the highest maximum wind speeds (≥ 20 m s^{-1}; mean of 12 m s^{-1}; Fig. S1), with 78 total days over the 12 yr of data experiencing winds ≥ 8.3 m s^{-1}. The 60–90° sector accounted for most winds (23% of observations) and highest wind speeds (maximum 37 m s^{-1}; mean 24 m s^{-1}; Fig. S1). This result indicates that trees in our study, growing on slopes facing northeast–southeast, regularly experienced winds up to 8.3–19.4 m s^{-1}, which other studies have found to be enough to alter carbon allocation in tree growth (Moulia & Combes, 2004; Nicoll *et al.*, 2008).

We then used the wind topographic exposure (EXPOS) model – since this model has been regularly used in the LEF (Boose *et al.*, 2004; Uriarte *et al.*, 2019; Hall *et al.*, 2020; Ankori-Karlinsky *et al.*, 2024) – to calculate chronic wind exposure based on angles of prevailing wind direction and topographic barriers using an ALS-derived digital elevation model (DEM, 30-m resolution) from NASA's March 2017 flights over Puerto Rico with Goddard's LiDAR, Hyperspectral, and Thermal (G-LiHT) Airborne Image sensor (Cook *et al.*, 2013). To assess exposure using EXPOS, we considered prevailing wind directions 60–120° (Fig. S1) and used an inflection angle of 15° (Batke *et al.*, 2014) and a maximum search distance (how far upwind a barrier matters) of 0.5 km, yielding a 30-m resolution binary wind exposure map for the LFDP (Fig. 1). Notably, the direction of chronic winds differs from most recent hurricane paths (see Uriarte *et al.*, 2019, for details), making our estimate of chronic winds independent from severe storm winds. To make sure the effects of chronic wind exposure were not confounded with variation in light availability due to aspect, we used the OCE package in R v.4.1.2 (R Core Team, 2021) to calculate the mean solar azimuth angle at noon during the peak growing season (June–August) in the LFDP (Kelley *et al.*, 2022) and ensured that the aspect for light availability was not correlated with that of wind exposure but instead orthogonal to it (Fig. S1). Note that our estimate of chronic wind exposure is topographically derived and independent of canopy structure, allowing us to examine wind-induced changes in tree architecture while avoiding circularity.

Tree sampling, geolocation, and crown segmentation

We focused our analyses on four common canopy tree species (Table 1) – the pioneer *C. schreberiana* Miq., secondary successional species *Buchenavia tetraphylla* Aubl. Howard, and two late-successional species: *D. excelsa* Vahl. and *M. bidentata* (*A.* DC.) Chev (Thompson *et al.*, 2002). These species vary substantially in lifespan – *B. tetraphylla* and *C. schreberiana* live between *c.* 70 and 30 yr, respectively, while *D. excelsa* and *M. bidentata* can live up to 400 yr (Burns & Honkala, 1990; Weaver, 1991). We chose these species since they account for *c.* 40% of the basal area of trees ≥ 10-cm dbh in the forest and vary in life-history strategies related to light use, recruitment, and wind resistance (Uriarte *et al.*, 2012). We randomly sampled individual trees ≥ 20 cm dbh from each species from the 2016 Census data, stratifying by our estimate of chronic wind exposure. Stratified random sampling was performed beforehand rather than in the field in order to reduce unintentional sampling bias. We chose

© 2025 The Author(s).
New Phytologist © 2025 New Phytologist Foundation. This article has been contributed to by U.S. Government employees and their work is in the public domain in the USA.

14698137, 0, Downloaded from https://nph.onlinelibrary.wiley.com/doi/10.1111/nph.70294 by Maria Uriarte - Columbia University Libraries , Wiley Online Library on [12/06/2025]. See the Terms and Conditions (https://onlinelibrary.wiley.com/terms-and-conditions) on Wiley Online Library for rules of use; OA articles are governed by the applicable Creative Commons License

Table 1 Target species in this study by chronic wind exposure.

Species	Wind exposure	No. of stems	dbh (cm)	Height (m)	Area (m^2)
Buchenavia tetraphylla	Protected	17	51.41 ± 4.5	26.6 ± 0.6	127.7 ± 20.1
(*c.* 70-yr lifespan)	Exposed	5	52.40 ± 4.6	23.9 ± 2.3	84.8 ± 25.3
Cecropia schreberiana	Protected	15	25.87 ± 1.6	22.6 ± 0.6	48.5 ± 9.3
(*c.* 30 to 70-yr lifespan)	Exposed	11	27.82 ± 1.7	21.9 ± 0.9	51.7 ± 6.7
Dacryodes excelsa	Protected	19	56.63 ± 2.7	26.5 ± 0.5	32 ± 3.5
(up to *c.* 400-yr lifespan)	Exposed	18	45.56 ± 3.3	22.9 ± 0.6	26.1 ± 3.5
Manilkara bidentata	Protected	27	43.30 ± 2.6	25.8 ± 0.7	39.6 ± 5.1
(up to *c.* 400-yr lifespan)	Exposed	12	40.25 ± 5.1	25.5 ± 1.2	35.7 ± 15.2

Sample size (no. of stems with full ALS data), and mean ± SE diameter at breast height (dbh), tree height, and crown area.

the 20-cm dbh threshold to ensure target trees were in the canopy and visible so that we could carry out crown segmentation using high-resolution photography and ALS data collected by G-LiHT. To avoid direct confounding effects of previous hurricanes on tree architecture, we only included trees with no previous record of severe (i.e. no tip-up, snap-off, and root break or bent) or moderate (i.e. branch breaks) hurricane damage dating back to 1989 (Uriarte *et al.*, 2019).

To connect field data to ALS-derived architecture for individual trees, we used a Geo7x handheld GPS device (Trimble Navigation Limited©, Westminster, CO, USA) with a spatial SE resolution of ±0.15 m with an antenna at 2-m aboveground to geolocate target trees in February 2022. For each tree, we placed the GPS device on the stem and measured points every second for 3 min (Fig. 1). We used the Differential Corrections function in the TRIMBLE PATHFINDER© software to precisely locate each tree stem, achieving a mean positional accuracy of 0.88 m (±0.05 m SE), and exported points as a shapefile. We then overlaid the measured tree location data with 0.03-m resolution red, green blue (RGB) raster images from G-LiHT (Cook *et al.*, 2013) to visually and manually segment crowns in the QGIS DESKTOP© software v.3.16.4 (Fig. 1), exporting the resultant polygon shapefile and creating a convex hull for each crown using the ALPHAHULL R package (Pateiro-Lopez & Rodriguez-Casal, 2022). We only segmented tree crowns that could be confidently identified in the RGB images (Fig. 1). This approach allowed us to compare topographically wind-exposed and -protected trees, but restricted our sample by excluding subcanopy trees. The final sample size included 124 trees (Table 1).

Tree architecture

To calculate tree architectural metrics, we aligned the segmented crown shapefile from the RGB images for each tree with ALS data from G-LiHT and created tree-specific point clouds with the LIDR R package, considering as part of the tree crown any ALS returns within the manually segmented convex hulls, cropping them vertically from the tallest ALS return to 5-m aboveground (Aubry-Kientz *et al.*, 2019; Roussel, 2021). ALS data had a mean sampling density of 12 laser pulses per m^2 (Cook *et al.*, 2013; Leitold *et al.*, 2021), above the 7–8 pulses m^{-2} recommended for quantifying vertical structure (LaRue *et al.*, 2022). We normalized point clouds by classifying ground terrain using the LIDR package and filtered them to only include first returns, representing vegetation (Roussel, 2021).

For individual tree metrics, we used the dbh recorded in the 2016 Census as stem size. We calculated tree height (m) as the highest value in the ALS returns for each segmented crown (Fig. S2). We then calculated slenderness for each tree as height dbh^{-1} (m). Crown area (m^2) for each tree was calculated for each convex hull using the RASTER R package (Hijmans *et al.*, 2021). We used the ALPHASHAPE3D R package to calculate the crown volume for each crown as the total number of ALS returns within the convex hull (Pateiro-Lopez & Rodriguez-Casal, 2022; Lafarge & Pateiro-Lopez, 2023).

Neighborhood variables

To assess potential confounding effects of topography and soil conditions on tree architecture, we used a 1-m resolution DEM (Cook *et al.*, 2013) and calculated the mean curvature, elevation, slope, and topographic wetness index in 20 m radius buffers around each tree (Quinn *et al.*, 1995; Muscarella *et al.*, 2020). We chose 20 m to replicate the scale of geolocation in the plot inventory, as well as neighborhood dynamics (Uriarte *et al.*, 2004; Hogan *et al.*, 2016).

Although we selected undamaged trees in previous hurricanes, trees growing near other trees that were damaged by hurricanes could indirectly alter the light conditions surrounding our target trees and, therefore, their biomass allocation. To account for indirect effects of hurricanes on neighborhood light conditions, we calculated the proportion of severely damaged stems from Hurricane Hugo in 20 m radius buffers around each tree (Walker, 1991). To account for neighborhood stem crowding, which may alter resource competition and growth of target trees, we calculated the neighborhood crowding index (NCI):

$$NCI_i = \sum_{j=1, i \neq j}^{J} \cdot \frac{dbh_j^2}{d_{i,j}^2} \qquad \text{Eqn 1}$$

where stem i has j neighbors within 20 m and $d_{i,j}$ is the distance in meters from stem i to neighbor j (Uriarte *et al.*, 2004). Note that we used the third LFDP census in 2000 (17 yr before ALS measurements) to evaluate how prior crowding may have affected long-term tree growth and allocation and therefore current architecture.

© 2025 The Author(s).
New Phytologist © 2025 New Phytologist Foundation. This article has been contributed to by U.S. Government employees and their work is in the public domain in the USA.

14698137, 0, Downloaded from https://nph.onlinelibrary.wiley.com/doi/10.1111/nph.70294 by Maria Uriarte - Columbia University Libraries , Wiley Online Library on [12/06/2025]. See the Terms and Conditions (https://onlinelibrary.wiley.com/terms-and-conditions) on Wiley Online Library for rules of use; OA articles are governed by the applicable Creative Commons License

14698137, 0, Downloaded from https://nph.onlinelibrary.wiley.com/doi/10.1111/nph.70294 by Maria Uriarte - Columbia University Libraries , Wiley Online Library on [12/06/2025]. See the Terms and Conditions (https://onlinelibrary.wiley.com/terms-and-conditions) on Wiley Online Library for rules of use; OA articles are governed by the applicable Creative Commons License

Wind vulnerability modeling

To understand how architectural changes from chronic wind exposure may affect a tree's mechanical vulnerability to wind-induced stem break, we estimated the wind vulnerability for each individual tree *i* of species *s* (vul_{is}) at storm speeds (e.g. 25 m s^{-1}) based on an established model for mechanical vulnerability to winds (Gardiner *et al.*, 2008; Quine *et al.*, 2021):

$$vul_{is} \sim \frac{H_{is}}{dbh_{is}^3} \cdot \frac{A_{is}}{\rho_s} \quad \text{Eqn 2}$$

where H is the vertical height of the tree in *m*, dbh is the diameter of the stem in cm at 1.3 m height (cubed to simulate a circular stem shape), A is the surface area of the crown in m^2, and ρ is the species wood density defined as the dry wood weight to volume in kg cm^{-3} (Gardiner *et al.*, 2000; Niklas & Spatz, 2010; Jackson *et al.*, 2021b). Wood density values were obtained from (Swenson *et al.*, 2012). This equation was derived from models that represent the effects of wind forces on tree mechanics, inducing stems to break (Quine & Gardiner, 2007; Gardiner *et al.*, 2008; Quine *et al.*, 2021). Additional details are provided in the Supporting Information (Notes S1).

Statistical analyses

We ran multiple linear regressions of estimated vulnerability as well as each individual tree architectural metric – height, slenderness, and crown area – as a function of chronic wind exposure, curvature, dbh (except in the regressions for slenderness and vulnerability, as dbh is used to calculate them), elevation, previous neighborhood hurricane damage, neighborhood crowding, slope, and topographic wetness within species in R (Bolker, 2008). To facilitate interpretation of results and compare effects of each covariate (as they differed substantially in scale), we used the *scale* function in R to standardize all predictors by subtracting the species-level mean and dividing by the SD. Before running regressions, we checked assumptions of normality for response variables (Shapiro & Wilk, 1965) and assessed multicollinearity of independent variables (Fig. S3), using a threshold of $r \leq 0.7$ and ≤ 5 for variance inflation (Dormann *et al.*, 2013). All models reported here met the conditions mentioned previously. To further avoid issues of multicollinearity due to our relatively small sample sizes, we used a model-selection approach with two-direction stepwise regression using Akaike's Information Criterion (AIC) to select the best model (Burnham & Anderson, 2002; Ripley *et al.*, 2022). Here, we report the best models, but details for the full models are available in the Tables S1 and S2.

Results

Overall species differences in tree architecture

We had expected longer-lived species to have taller stems and larger crown areas. We found partial support for this pattern. The pioneer *C. schreberiana* was shorter by *c.* 4 m on average than other species (Table 1; Fig. 2a,b). However, it had larger crown areas than other species (Table 1; Fig. 2c). *B. tetraphylla* had the tallest, largest crowns, while *D. excelsa* and *M. bidentata* trees were intermediate in height and crown architecture (Table 1; Figs 2a,c, S2). Consequently, allometric relationships differed significantly between species (Fig. S4), with only *B. tetraphylla* and *M. bidentata* aligning with allometric relationships previously derived for tropical trees (Jucker *et al.*, 2017).

Chronic wind effects on within-species tree architecture

We had hypothesized that trees exposed to chronic winds would grow less slender stems and smaller crown areas. We found strong

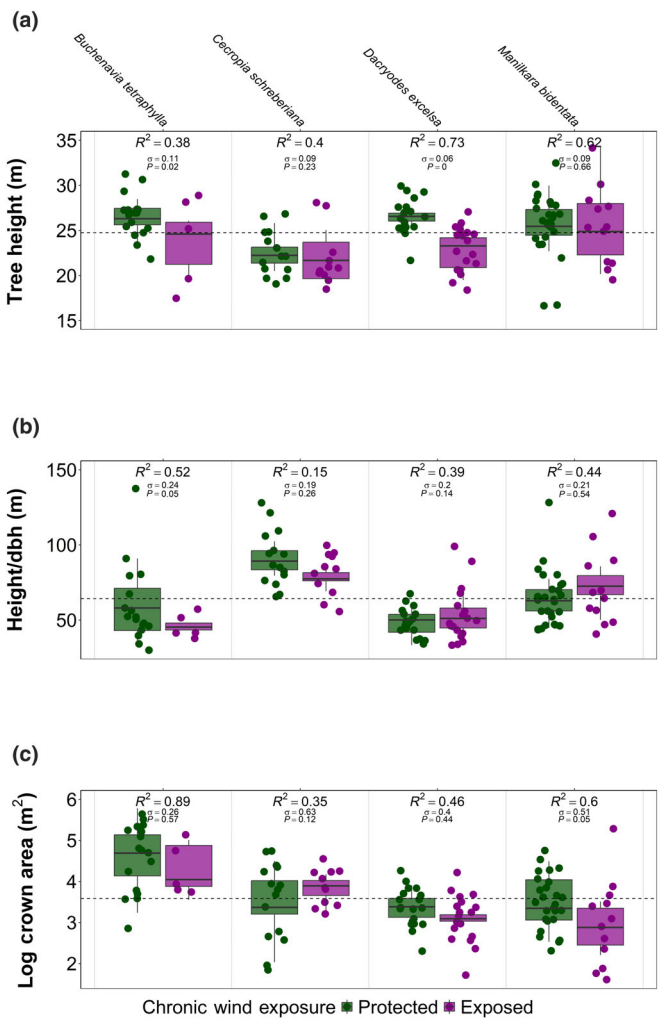

Fig. 2 Impacts of chronic wind exposure (color legend) on tree architecture of 124 trees of four common species, *Buchenavia tetraphylla, Cecropia schreberiana, Dacryodes excelsa, Manilkara bidentata*, in the Luquillo Forest Dynamics Plot: (a) tree height (m), (b) tree slenderness (height/diameter at breast height (dbh), m), (c) crown area (m^2). Note that crown area is natural log-transformed for easier visualization. Points represent observed individual tree data; boxplots represent model median and interquartile-range predictions, and the dotted line represents mean values for all species. R^2 and error (sigma) values are from the model fit, and *P*-values indicate significance of chronic wind exposure effect.

© 2025 The Author(s).
New Phytologist © 2025 New Phytologist Foundation. This article has been contributed to by U.S. Government employees and their work is in the public domain in the USA.

support for this: chronic wind exposure significantly reduced height in *D. excelsa* and slenderness in *B. tetraphylla* (Fig. 2a,b; Tables 2, 3, S1, S2), and significantly reduced crown areas in *B. tetraphylla, D. excelsa*, and *M. bidentata* (Fig. 2c; Tables 2, S1). Compared with protected trees, wind-exposed *B. tetraphylla* trees had 42-m^2 smaller crown areas, were 2.7 m shorter, and 20% less slender; wind-exposed *D. excelsa* trees were 3.6 m shorter, and wind-exposed *M. bidentata* trees had 4-m^2 or 14% smaller crown areas (Fig. 2; Tables 1, S1). On the other hand, *C. schreberiana* – the shortest-lived and fastest-growing species in our dataset – showed no architectural difference between chronically wind-exposed and sheltered trees. Importantly, chronic wind effects on tree architecture were still pronounced independent of other environmental effects, per the statistical analyses (Tables 2, 3, S1, S2).

Prior hurricane, neighborhood, and topographic effects on tree architecture

Previous neighborhood-scale disturbances had perceptible effects on tree architecture. Trees growing in stands previously severely damaged by hurricane Hugo were shorter and less slender (Tables 2, 3, S1, S2). However, *C. schreberiana* trees in damaged areas grew larger crown areas (Tables 2, S1). Neighborhood stem crowding, on the other hand, had weak effects on tree architecture (Tables 2, 3, S1, S2).

Topographical variables also had significant, but inconsistent, effects on tree architecture. Both *B. tetraphylla* and *D. excelsa* grew shorter in valleys than in ridges (in terms of slope angle and not aspect), and *D. excelsa* grew taller on steeper slopes and had larger crowns in water-saturated soils (Tables 2, 3, S1, S2). Variation in elevation did not have significant effects on tree architecture.

Species and wind-induced differences in mechanical vulnerability

Overall species differences in architecture were reflected in estimated mechanical vulnerability to severe winds – *B. tetraphylla* and *C. schreberiana* trees had the highest wind vulnerability due to lower wood density in *C. schreberiana* and larger crown areas in *B. tetraphylla* (Figs 2c, 3).

Architectural changes from chronic winds significantly affected estimated wind vulnerability in all species except for *C. schreberiana* (Fig. 3; Tables 2, 3). This effect resulted in the lowest estimated vulnerability for chronically wind-exposed *D. excelsa* trees, which had a 24% reduction in estimated vulnerability compared with wind-protected *D. excelsa* trees (Fig. 3).

Cecropia schreberiana trees grew larger crowns when growing in neighborhoods severely damaged by hurricane Hugo (Tables 2, S1), resulting in higher estimated vulnerability for trees in those stands (Tables 3, S2). Similarly, *M. bidentata* trees grew more slender and bigger crowns on steeper slopes, also resulting in increased estimated vulnerability for those trees (Tables 3, S2).

Table 2 Results of best multiple linear regression models for height and crown area for four species.

	Height				Crown area			
	BUCTET	*CECSCH*	*DACEXC*	*MANBID*	*BUCTET*	*CECSCH*	*DACEXC*	*MANBID*
(Intercept)	3.28 (0.03)***	3.12 (0.02)***	3.23 (0.02)***	3.23 (0.02)***	4.53 (0.07)***	3.48 (0.17)***	3.31 (0.11)***	3.44 (0.10)***
Wind exposure	−0.15 (0.06)*	−0.05 (0.04)	−0.11 (0.03)***	0.02 (0.04)	−0.09 (0.15)	0.45 (0.28)	−0.14 (0.18)	−0.37 (0.18)*
dbh	0.05 (0.02)	0.05 (0.02)*	0.04 (0.01)*	0.11 (0.02)***	0.58 (0.07)***	0.38 (0.14)*	0.45 (0.08)***	0.60 (0.08)***
Height					0.20 (0.07)*		−0.25 (0.09)*	
Crown area			−0.02 (0.01)					
Curvature	−0.09 (0.03)*		−0.07 (0.02)***	−0.09 (0.03)*		−0.29 (0.20)		
Elevation			0.02 (0.01)		−0.19 (0.06)**			
Slope		0.03 (0.02)	0.08 (0.01)***	0.03 (0.02)		−0.25 (0.17)		
TWI	−0.07 (0.03)*	0.06 (0.02)*				−0.32 (0.19)	0.21 (0.08)**	
Hugo damage			−0.03 (0.01)*	−0.08 (0.02)***		0.35 (0.13)*		
NCI	0.01 (0.02)			−0.03 (0.02)				
R^2 Adj.	0.38	0.39	0.73	0.62	0.88	0.35	0.45	0.59
RMSE	0.09	0.08	0.06	0.09	0.23	0.54	0.37	0.49
AIC	114.0	117.3	145.6	186.1	208.4	248.7	283.8	323.3

Each row indicates the parameter estimate for each predictor, with SE in parentheses, and statistical significance indicated by asterisks, where *P*-values = 0 '***' 0.001 '**' 0.01 '*' 0.05. Model performance statistics at the bottom. AIC indicating best model compared to full model (Supporting Information Table S1). Note that dependent variables were log-transformed. AIC, Akaike Information Criterion; *BUCTET*, *Buchenavia tetraphylla*; *CECSCH*, *Cecropia schreberiana*; *DACEXC*, *Dacryodes excelsa*; dbh, diameter at breast height; *MANBID*, *Manilkara bidentata*; NCI, Neighborhood crowding index; R^2 Adj., Adjusted coefficient of determination; RMSE, root-square mean model error; TWI, topographic wetness index.

New Phytologist © 2025 New Phytologist Foundation. This article has been contributed to by U.S. Government employees and their work is in the public domain in the USA.

© 2025 The Author(s).

14698137, 0, Downloaded from https://nph.onlinelibrary.wiley.com/doi/10.1111/nph.70294 by Maria Uriarte - Columbia University Libraries , Wiley Online Library on [12/06/2025]. See the Terms and Conditions (https://onlinelibrary.wiley.com/terms-and-conditions) on Wiley Online Library for rules of use; OA articles are governed by the applicable Creative Commons License

14698137, 0, Downloaded from https://nph.onlinelibrary.wiley.com/doi/10.1111/nph.70294 by Maria Uriarte - Columbia University Libraries , Wiley Online Library on [12/06/2025]. See the Terms and Conditions (https://onlinelibrary.wiley.com/terms-and-conditions) on Wiley Online Library for rules of use; OA articles are governed by the applicable Creative Commons License

Table 3 Results of best multiple linear regression models for slenderness (height/diameter at breast height) and estimated wind vulnerability for four species.

	Slender				Vulnerable			
	BUCTET	*CECSCH*	*DACEXC*	*MANBID*	*BUCTET*	*CECSCH*	*DACEXC*	*MANBID*
(Intercept)	4.043 (0.06)***	4.48 (0.05)***	3.83 (0.05)***	4.14 (0.04)***	−0.17 (0.02)***	0.09 (0.03)**	−0.26 (0.02)***	−0.53 (0.05)***
Wind exposure	−0.32 (0.16)*	−0.09 (0.08)	0.12 (0.08)	0.05 (0.07)	−0.12 (0.05)*	0.07 (0.04)	−0.11 (0.03)**	−0.18 (0.08)*
Crown area	−2.9 (0.16)***	−0.6 0.04	−0.13 (0.04)**	−0.14 (0.04)***				
Curvature	−0.08 (0.06)		−0.13 (0.05)**		−0.10 (0.03)**	−0.05 (0.02)*		−0.06 (0.04)
Elevation			0.05 (0.04)		−0.07 (0.03)*			0.06 (0.04)
Slope	0.10 (0.07)		0.08 (0.05)				0.03 (0.02)	0.10 (0.04)*
TWI					−0.06 (0.03)		0.03 (0.02)	
Hurricane Hugo	−0.01 (0.08)	0.06 (0.05)	−0.01 (0.04)	−0.12 (0.04)***		0.04 (0.02)*		−0.07 (0.04)
NCI				−0.04 (0.02)				
R^2 Adj.	0.52	0.15	0.39	0.44	0.36	0.22	0.27	0.17
RMSE	0.20	0.17	0.18	0.2-	0.09	0.09	0.09	0.22
AIC	181.9	223.9	282.7	319.3	−41.1	−36.4	−89.0	−39.8

Each row indicates the parameter estimate for each predictor, with SE in parentheses, and statistical significance indicated by asterisks, where *P*-values = 0 '***' 0.001 '**' 0.01 '*' 0.05. Model performance statistics at the bottom. AIC indicating best model compared to full model (Supporting Information Table S2). Note that dependent variables were log-transformed. AIC, Akaike Information Criterion; *BUCTET*, *Buchenavia tetraphylla*; *CECSCH*, *Cecropia schreberiana*; *DACEXC*, *Dacryodes excelsa*; *MANBID*, *Manilkara bidentata*; NCI, Neighborhood crowding index; R^2 Adj., Adjusted coefficient of determination; RMSE, root-square mean model error; TWI, topographic wetness index.

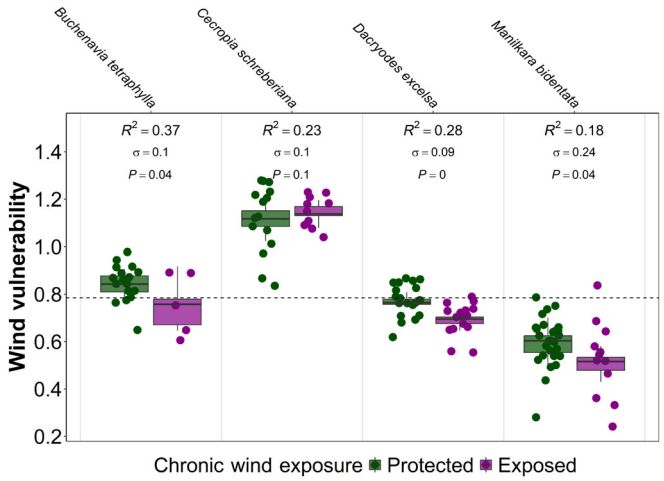

Fig. 3 Relationship between chronic wind exposure (color legend) and estimated wind vulnerability for 124 trees of four common species, *Buchenavia tetraphylla, Cecropia schreberiana, Dacryodes excelsa, Manilkara bidentata*, in the Luquillo Forest Dynamics Plot: points represent observed individual tree data; boxplots represent medians and interquartile ranges; and the dotted line represents mean values for all species. R^2 and error (sigma) values are from the model fit, and *P*-values indicate significance of chronic wind exposure effect.

Discussion

Working in a tropical forest with predictable chronic wind directions, our study used a novel combination of high-resolution airborne remote sensing and long-term forest inventory data to show that chronic wind exposure leads to architectural changes in individual tropical forest trees of abundant species. Long-lived species in chronic winds grew less slender stems and smaller crowns, resulting in reductions in their estimated mechanical vulnerability to severe winds. Although our sample size and number of species were limited, our findings demonstrate that, even in a complex tropical forest and after accounting for multiple effects, directional wind exposure can lead to significant changes in adult tree architecture and mechanical vulnerability, and potentially forest dynamics in response to severe disturbances.

Chronic winds lead to architectural changes on tropical trees

We found evidence that tropical trees with higher exposure to chronic winds grew shorter and had smaller crowns. This effect differed across species, with shorter-lived species showing no evidence of wind-induced acclimation. Although a sample of four species requires care in interpretation, it is noteworthy that the two species that showed the biggest effect sizes in wind-induced acclimation – *D. excelsa* and *M. bidentata* – are also among the most resistant to hurricane-induced damage in Puerto Rico (Canham *et al.*, 2010; Uriarte *et al.*, 2019).

There are a number of possible mechanisms to explain species differences in wind-induced architectural changes: shorter pioneer species may be sheltered from wind effects by taller neighbors (Gardiner *et al.*, 2016); long-lived wind-exposed trees may invest in radial, belowground, or denser wood at the expense of primary growth to increase mechanical stability (Brüchert & Gardiner, 2006; Nicoll *et al.*, 2008; Bonnesoeur *et al.*, 2016; Niklas, 2016); or wind-exposed trees (regardless of life-history strategies) may lose crown biomass from branch damage or defoliation (Markham & Fernández Otárola, 2020). These possible mechanisms are discussed later.

Species differences in chronic wind-induced architectural changes may reflect neighborhood sheltering by taller trees. Trees of the pioneer species, *C. schreberiana*, were the shortest in our

© 2025 The Author(s).
New Phytologist © 2025 New Phytologist Foundation. This article has been contributed to by U.S. Government employees and their work is in the public domain in the USA.

dataset, and their architectural metrics did not vary based on chronic wind exposure. Conversely, longer-lived and taller species – *B. tetraphylla*, *D. excelsa*, and *M. bidentata* (Thompson *et al.*, 2002) – displayed evidence of wind-induced growth responses. These lines of evidence support findings from temperate forests – wind-induced structural variation may only occur if an exposed canopy tree lives long enough to experience significant strain (Hale *et al.*, 2012; MacFarlane & Kane, 2017).

Experiments have shown that trees exposed to chronic winds may also reduce their vulnerability to stem breaks by prioritizing stem diameter growth (Bonnesoeur *et al.*, 2016; Nicoll *et al.*, 2019). Indeed, trees exposed to chronic winds in our study were shorter on average than protected trees for a given stem diameter. However, we found no direct evidence of difference in trees' stem diameter growth over the 30 yr of census data based on chronic wind exposure (data not shown). It is possible our sampling scheme rendered us unable to examine such mechanisms: we sampled canopy trees > 20-cm dbh, which, apart from *C. schreberiana*, tend to be decades old by the time they reach this size and may have reduced growth rates at the time of measurement (Fahey *et al.*, 2015). Wind-exposed trees may have also invested in denser wood, regardless of diameter growth (Asner & Goldstein, 1997; Angulo-Sandoval & Aide, 2000), although the two are usually correlated (Gardiner *et al.*, 2016). Another possibility is that trees altered their branching architecture – perhaps streamlining with chronic winds – or invested differently in their leaf shape and area (Markham & Fernández Otárola, 2020). Unfortunately, without terrestrial laser scanning (TLS) data, we are limited in our ability to quantify branching architecture, and we currently have no wood density data for different levels of chronic wind exposure to evaluate this hypothesis.

Chronic winds may also lead to shorter trees and smaller crowns through trade-offs of increased carbon allocation to root systems (Basnet *et al.*, 1993). Indeed, past research in the LEF has found that *D. excelsa* trees have the deepest roots of all species studied (Yaffar *et al.*, 2019; Yaffar & Norby, 2020), and root grafting in this species has been tentatively tied to high resistance to hurricane damage (Basnet *et al.*, 1992). These studies suggest that differential carbon allocation to roots may be responsible for the significant reductions in height and crown area we observed in chronically wind-exposed *D. excelsa* and *M. bidentata* trees. Unfortunately, the difficulty in obtaining species-specific root data means we have no data to directly evaluate this hypothesis.

Differences in architecture based on chronic winds may also be caused by branch damage or defoliation (Haber *et al.*, 2020). None of the trees in our study were damaged by previous hurricanes dating back to 1989, suggesting that biomass loss from storms may not be primarily responsible for the reductions in crown metrics we observed in wind-exposed trees. However, field data every 5 yr do not collect damage from nonhurricane storms, and annual remote satellite sensors are not available at tree-level resolutions, leaving us unable to assess the importance of this mechanism in driving structural changes (Peterson, 2019; Markham & Fernández Otárola, 2020). However, the growing availability of multiple ALS flyovers would allow future researchers to track damage rates from nonsevere storms to differentiate between mechanisms of damage and allocation.

Disturbances leave decades-long architectural legacies

Higher light conditions following hurricanes can often lead to increased growth and thus taller, larger tree crowns (Zimmerman *et al.*, 2014). Contrary to such expectations, higher surrounding damage in our study did not correlate with increases in height. In fact, *D. excelsa* and *M. bidentata* were shorter in stands with more previous damage, while *C. schreberiana* did not differ in height but grew larger crown areas in such stands. These findings may make sense in terms of community responses to severe disturbances, in which recovery involves extremely high recruitment and growth rates of understory trees and pioneer species (Van Bloem *et al.*, 2006; Chevalier *et al.*, 2022; Zhang *et al.*, 2022). It may be that in highly damaged stands, the higher light conditions in horizontal space reduced vertical competition for light (Loehle, 2000; Strigul *et al.*, 2008) so that trees invested in growing wider crowns to capture available light rather than growing taller. Another possibility is that indirect damage from hurricane Hugo not captured by our data may have shortened trees in highly damaged stands (Atkins *et al.*, 2020). Regardless, although our limited sample size makes it difficult to extrapolate, it is worth noting that even in tall, long-lived canopy trees individually undamaged by Hugo in 1989, surrounding neighborhood damage appeared to leave observable architectural legacies 30 yr after the storm.

Species responses to chronic winds map onto hurricane resistance strategies

Tree species in hurricane-prone forests across the Caribbean have evolved different strategies to survive and regenerate after hurricanes, which make landfall on the island in multidecadal intervals (Boose *et al.*, 2004; Canham *et al.*, 2010; Zimmerman *et al.*, 2021). Pioneer species such as *C. schreberiana* are highly vulnerable to damage but regenerate rapidly (Canham *et al.*, 2010; Uriarte *et al.*, 2012), whereas longer-lived species such as *M. bidentata* and *D. excelsa* have much lower rates of damage (Uriarte *et al.*, 2019; Taylor *et al.*, 2023), with *B. tetraphylla* falling somewhere in between (Uriarte *et al.*, 2019). Our study shows that species differences in chronic wind-induced architectural metrics reflect these life-history strategies. For example, *C. schreberiana* grows fast at the expense of increased vulnerability to severe storms (Smith-Martin *et al.*, 2022), which fits with our findings of its higher wind vulnerability compared with other species, regardless of chronic winds. Conversely, the reduced height in wind-exposed *D. excelsa* trees and the smaller crown areas in wind-exposed *M. bidentata* trees suggest acclimation strategies to reduce vulnerability to more severe storms. The risk of damage from severe winds consistently increases with tree height (Jackson *et al.*, 2019a; Hall *et al.*, 2020). Since wind-exposed *D. excelsa* trees in our study were *c.* 3 m shorter on average than protected trees, the chronically wind-exposed trees may

© 2025 The Author(s).
New Phytologist © 2025 New Phytologist Foundation. This article has been contributed to by U.S. Government employees and their work is in the public domain in the USA.

14698137, 0, Downloaded from https://nph.onlinelibrary.wiley.com/doi/10.1111/nph.70294 by Maria Uriarte - Columbia University Libraries , Wiley Online Library on [12/06/2025]. See the Terms and Conditions (https://onlinelibrary.wiley.com/terms-and-conditions) on Wiley Online Library for rules of use; OA articles are governed by the applicable Creative Commons License

be significantly less susceptible to damage from future hurricanes. Additionally, if the wind-induced effect we observe is driven by carbon allocation to denser wood or more extensive root systems, then nonsevere winds may lead to growth changes that allow trees to better resist severe storms. Future studies could test this possibility by monitoring wind-induced differences in wood density and belowground biomass, and compare those with rates of damage from hurricanes. The increasing availability of multi- and hyperspectral sensors alongside TLS or ALS data can dramatically expand data acquisition of *in situ* tree architecture, and help answer some of these remaining questions (Jackson *et al.*, 2019b; Reilly *et al.*, 2021; Gao *et al.*, 2022).

Acknowledgements

Collection of tree data was supported by NSF DEB-1546686, DEB-0516066, BSR-8811902, DEB-9411973, DEB-0080538, DEB-0218039, DEB-0620910, and DEB-0963447 to the University of Puerto Rico, working with the International Institute of Tropical Forestry (USDA Forest Service), for the Luquillo Long-Term Ecological Research Program. TJ was supported by the UK Natural Environment Research Council NE/S010750/1 and NE/X000281/1. Goddard's LiDAR, Hyperspectral, and Thermal (G-LiHT) data collection was supported by the US Department of Energy Next Generation Ecosystem Experiment-Tropics Project and the USDA Forest Service International Institute for Tropical Forestry (IITF). DM was supported by the US Department of Energy Terrestrial Ecosystem Science Program, Interagency Agreements with NASA no. 89243018SSC000013. We would like to thank the valuable feedback from the anonymous reviewers. We would like to thank Dr Chengliang Tang for providing excellent feedback and suggestions. We would also like to thank the numerous field technicians and assistants who worked on the 2016 census, as well as Nina Berinstein, Isabela Brown, Ali Malik, Monique Picon, Melissa Salva Sauri, and Dr Naima Starkloff for assisting with the 2022 field campaign, and Dr Bruce Cook and Dr Sebastian Martinuzzi for assisting with planning and executing the 2017 G-LiHT airborne campaign.

Competing interests

None declared.

Author contributions

RA-K and MU conceived the ideas and designed the methodology. RA-K, JKZ, GY, TZ and DCM collected the data. RA-K, TDJ and GY analyzed the data. RA-K and MU led the writing of the manuscript. All authors contributed critically to the drafts and gave final approval for publication.

ORCID

Roi Ankori-Karlinsky https://orcid.org/0000-0002-8277-8136
Tobias D. Jackson https://orcid.org/0000-0001-8143-6161

Data availability

Data are available on Dryad doi: 10.5061/dryad.zw3r228fq.

References

Angulo-Sandoval P, Aide TM. 2000. Effect of plant density and light availability on leaf damage in Manilkara bidentata (Sapotaceae). *Journal of Tropical Ecology* **16**: 447–464.

Ankori-Karlinsky R, Hall J, Murphy L, Muscarella R, Martinuzzi S, Fahey R, Zimmerman JK, Uriarte M. 2024. Chronic winds reduce tropical forest structural complexity regardless of climate, topography, or forest age. *Ecosystems* **27**: 479–491.

Anyomi KA, Mitchell SJ, Ruel J-C. 2016. Windthrow modelling in old-growth and multi-layered boreal forests. *Ecological Modelling* **327**: 105–114.

Asner GP, Goldstein G. 1997. Correlating stem biomechanical properties of Hawaiian canopy trees with hurricane wind damage. *Biotropica* **29**: 145–150.

Atkins JW, Bond-Lamberty B, Fahey RT, Haber LT, Stuart-Haëntjens E, Hardiman BS, LaRue E, McNeil BE, Orwig DA, Stovall AEL *et al.* 2020. Application of multidimensional structural characterization to detect and describe moderate forest disturbance. *Ecosphere* **11**: e03156.

Aubry-Kientz M, Dutrieux R, Ferraz A, Saatchi S, Hamraz H, Williams J, Coomes D, Piboule A, Vincent G. 2019. A comparative assessment of the performance of individual tree crowns delineation algorithms from als data in tropical forests. *Remote Sensing* **11**: 1086.

Basnet K. 1992. Effect of topography on the pattern of trees in Tabonuco (*Dacryodes excelsa*) dominated rain forest of Puerto Rico. *Biotropica* **24**: 31–42.

Basnet K, Likens GE, Scatena FN, Lugo AE. 1992. Hurricane Hugo: damage to a tropical rain forest in Puerto Rico. *Journal of Tropical Ecology* **8**: 47–55.

Basnet K, Scatena FN, Likens GE, Lugo AE. 1993. Ecological consequences of root grafting in tabonuco (*Dacryodes excelsa*) trees in the Luquillo experimental forest, Puerto Rico. *Biotropica* **25**: 28–35.

Batke SP, Jocque M, Kelly DL. 2014. Modelling hurricane exposure and wind speed on a mesoclimate scale: a case study from Cusuco NP, Honduras. *PLoS ONE* **9**: e91306.

Bolker BM. 2008. *Ecological models and data in R.* Princeton, NJ, USA: Princeton University Press.

Bonnesoeur V, Constant T, Moulia B, Fournier M. 2016. Forest trees filter chronic wind-signals to acclimate to high winds. *New Phytologist* **210**: 850–860.

Boose ER, Serrano MI, Foster DR. 2004. Landscape and regional impacts of hurricanes in Puerto Rico. *Ecological Monographs* **74**: 335–352.

Boudreault L-É, Bechmann A, Tarvainen L, Klemedtsson L, Shendryk I, Dellwik E. 2015. A LiDAR method of canopy structure retrieval for wind modeling of heterogeneous forests. *Agricultural and Forest Meteorology* **201**: 86–97.

Brüchert F, Gardiner B. 2006. The effect of wind exposure on the tree aerial architecture and biomechanics of Sitka spruce (*Picea sitchensis*, Pinaceae). *American Journal of Botany* **93**: 1512–1521.

Burnham KP, Anderson DR. 2002. *Model selection and multimodel inference: a practical information-theoretic approach.* New York, NY, USA: Springer-Verlag.

Burns RM, Honkala BH. 1990. *Silvics of North America: vol. 2.* Washington, DC, USA: United States Department of Agriculture (USDA), Forest Service, Agriculture Handbook.

Canham CD, Thompson J, Zimmerman JK, Uriarte M. 2010. Variation in susceptibility to hurricane damage as a function of storm intensity in Puerto Rican tree species. *Biotropica* **42**: 87–94.

Chevalier H, Brokaw NVL, Ward SE, Zimmerman JK, Shiels AB, Bithorn J, Matta Carmona S. 2022. Aboveground carbon responses to experimental and natural hurricane impacts in a subtropical wet forest in Puerto Rico. *Ecosphere* **13**: e4041.

Cook BD, Corp LA, Nelson RF, Middleton EM, Morton DC, McCorkel JT, Masek JG, Ranson KJ, Ly V, Montesano PM. 2013. NASA Goddard's LiDAR, hyperspectral and thermal (G-LiHT) airborne imager. *Remote Sensing* **5**: 4045–4066.

Coomes DA, Šafka D, Shepherd J, Dalponte M, Holdaway R. 2018. Airborne laser scanning of natural forests in New Zealand reveals the influences of wind on forest carbon. *Forest Ecosystems* **5**: 10.

© 2025 The Author(s).
New Phytologist © 2025 New Phytologist Foundation. This article has been contributed to by U.S. Government employees and their work is in the public domain in the USA.

14698137, 0, Downloaded from https://nph.onlinelibrary.wiley.com/doi/10.1111/nph.70294 by Maria Uriarte - Columbia University Libraries , Wiley Online Library on [12/06/2025]. See the Terms and Conditions (https://onlinelibrary.wiley.com/terms-and-conditions) on Wiley Online Library for rules of use; OA articles are governed by the applicable Creative Commons License

Cremer KW, Borough CJ, McKinnell FH, Carter PR. 1982. Effects of stocking and thinning on wind damage in plantations. *New Zealand Journal of Forestry Science* **12**: 244–268.

Dormann CF, Elith J, Bacher S, Buchmann C, Carl G, Carré G, Marquéz JRG, Gruber B, Lafourcade B, Leitão PJ *et al.* 2013. Collinearity: a review of methods to deal with it and a simulation study evaluating their performance. *Ecography* **36**: 27–46.

Ennos AR. 1997. Wind as an ecological factor. *Trends in Ecology & Evolution* **12**: 108–111.

Fahey RT, Fotis AT, Woods KD. 2015. Quantifying canopy complexity and effects on productivity and resilience in late-successional hemlock-hardwood forests. *Ecological Applications: A Publication of the Ecological Society of America* **25**: 834–847.

Flynn DFB, Uriarte M, Crk T, Pascarella JB, Zimmerman JK, Aide TM, Ortiz MAC. 2010. Hurricane disturbance alters secondary forest recovery in Puerto Rico. *Biotropica* **42**: 149–157.

Fortunel C, Lasky JR, Uriarte M, Valencia R, Wright SJ, Garwood NC, Kraft NJB. 2018. Topography and neighborhood crowding can interact to shape species growth and distribution in a diverse Amazonian forest. *Ecology* **99**: 2272–2283.

Gao L, Chai G, Zhang X. 2022. Above-ground biomass estimation of plantation with different tree species using airborne lidar and hyperspectral data. *Remote Sensing* **14**: 2568.

Gardiner B, Berry P, Moulia B. 2016. Review: wind impacts on plant growth, mechanics and damage. *Plant Science* **245**: 94–118.

Gardiner B, Byrne K, Hale S, Kamimura K, Mitchell SJ, Peltola H, Ruel J-C. 2008. A review of mechanistic modelling of wind damage risk to forests. *Forestry* **81**: 447–463.

Gardiner B, Peltola H, Kellomäki S. 2000. Comparison of two models for predicting the critical wind speeds required to damage coniferous trees. *Ecological Modelling* **129**: 1–23.

Gelder HAV, Poorter L, Sterck FJ. 2006. Wood mechanics, allometry, and life-history variation in a tropical rain forest tree community. *New Phytologist* **171**: 367–378.

Gorgens EB, Nunes MH, Jackson T, Coomes D, Keller M, Reis CR, Valbuena R, Rosette J, Almeida DRA, Gimenez B *et al.* 2021. Resource availability and disturbance shape maximum tree height across the Amazon. *Global Change Biology* **27**: 177–189.

Haber LT, Fahey RT, UK SB, Pascuas NC, Currie WS, Hardiman BS, Gough CM. 2020. Forest structure, diversity, and primary production in relation to disturbance severity. *Ecology and Evolution* **10**: 4419–4430.

Hale SE, Gardiner BA, Wellpott A, Nicoll BC, Achim A. 2012. Wind loading of trees: influence of tree size and competition. *European Journal of Forest Research* **131**: 203–217.

Hall J, Muscarella R, Quebbeman A, Arellano G, Thompson J, Zimmerman JK, Uriarte M. 2020. Hurricane-induced rainfall is a stronger predictor of tropical forest damage in Puerto Rico than maximum wind speeds. *Scientific Reports* **10**: 4318.

Heartsill Scalley T. 2017. Insights on forest structure and composition from long-term research in the Luquillo mountains. *Forests* **8**: 204.

Hijmans RJ, Etten J, Sumner M, Cheng J, Baston D, Bevan A, Bivand R, Busetto L, Canty M, Fasoli B. 2021. RASTER: geographic data analysis and modeling. [WWW document] URL https://CRAN.R-project.org/package=raster.

Hogan JA, Zimmerman JK, Thompson J, Nytch CJ, Uriarte M. 2016. The interaction of land-use legacies and hurricane disturbance in subtropical wet forest: twenty-one years of change. *Ecosphere* **7**: e01405.

Jackson T, Sethi S, Dellwik E, Angelou N, Bunce A, van Emmerik T, Duperat M, Ruel J-C, Wellpott A, Van Bloem S *et al.* 2021a. The motion of trees in the wind: a data synthesis. *Biogeosciences* **18**: 4059–4072.

Jackson T, Shenkin A, Kalyan B, Zionts J, Calders K, Origo N, Disney M, Burt A, Raumonen P, Malhi Y. 2019a. A new architectural perspective on wind damage in a natural forest. *Frontiers in Forests and Global Change* **1**: 1303.

Jackson T, Shenkin A, Wellpott A, Calders K, Origo N, Disney M, Burt A, Raumonen P, Gardiner B, Herold M *et al.* 2019b. Finite element analysis of trees in the wind based on terrestrial laser scanning data. *Agricultural and Forest Meteorology* **265**: 137–144.

Jackson T, Shenkin AF, Majalap N, Jami JB, Sailim AB, Reynolds G, Coomes DA, Chandler CJ, Boyd DS, Burt A *et al.* 2021b. The mechanical stability of the world's tallest broadleaf trees. *Biotropica* **53**: 110–120.

Jackson TD, Bittencourt P, Poffley J, Anderson J, Muller-Landau HC, Ramos PAR, Rowland L, Coomes D. 2024. Wind shapes the growth strategies of trees in a tropical forest. *Ecology Letters* **27**: e14527.

Jaffe MJ. 1973. Thigmomorphogenesis: the response of plant growth and development to mechanical stimulation. *Planta* **114**: 143–157.

Johnston MH. 1992. Soil–vegetation relationships in a tabonuco forest community in the Luquillo Mountains of Puerto Rico. *Journal of Tropical Ecology* **8**: 253–263.

Jucker T. 2022. Deciphering the fingerprint of disturbance on the three-dimensional structure of the world's forests. *New Phytologist* **233**: 612–617.

Jucker T, Caspersen J, Chave J, Antin C, Barbier N, Bongers F, Dalponte M, Ewijk KY, Forrester DI, Haeni M *et al.* 2017. Allometric equations for integrating remote sensing imagery into forest monitoring programmes. *Global Change Biology* **23**: 177–190.

Kelley D, Richards C, Layton C. 2022. OCE: analysis of oceanographic data. [WWW document] URL https://CRAN.R-project.org/package=oce.

Lafarge T, Pateiro-Lopez B. 2023. ALPHASHAPE3D: implementation of the 3d alpha-shape for the reconstruction of 3d sets from a point cloud. [WWW document] URL https://CRAN.R-project.org/package=alphashape3d.

LaRue EA, Fahey R, Fuson TL, Foster JR, Matthes JH, Krause K, Hardiman BS. 2022. Evaluating the sensitivity of forest structural diversity characterization to LiDAR point density. *Ecosphere* **13**: e4209.

LaRue EA, Fahey RT, Alveshere BC, Atkins JW, Bhatt P, Buma B, Chen A, Cousins S, Elliott JM, Elmore AJ *et al.* 2023. A theoretical framework for the ecological role of three-dimensional structural diversity. *Frontiers in Ecology and the Environment* **21**: 4–13.

LaRue EA, Wagner FW, Fei S, Atkins JW, Fahey RT, Gough CM, Hardiman BS. 2020. Compatibility of aerial and terrestrial LiDAR for quantifying forest structural diversity. *Remote Sensing* **12**: 1407.

Leitold V, Morton DC, Martinuzzi S, Paynter I, Uriarte M, Keller M, Ferraz A, Cook BD, Corp LA, González G. 2021. Tracking the rates and mechanisms of canopy damage and recovery following hurricane maria using multitemporal lidar data. *Ecosystems* **25**: 4568.

Lin T-C, Hogan JA, Chang C-T. 2020. Tropical cyclone ecology: a scale-link perspective. *Trends in Ecology & Evolution* **20**: 12689.

Lines ER, Fischer FJ, Owen HJF, Jucker T. 2022. The shape of trees: reimagining forest ecology in three dimensions with remote sensing. *Journal of Ecology* **110**: 1730–1745.

Loehle C. 2000. Strategy space and the disturbance spectrum: a life-history model for tree species coexistence. *The American Naturalist* **156**: 14–33.

MacFarlane DW, Kane B. 2017. Neighbour effects on tree architecture: functional trade-offs balancing crown competitiveness with wind resistance. *Functional Ecology* **31**: 1624–1636.

Malhi Y, Jackson T, Patrick Bentley L, Lau A, Shenkin A, Herold M, Calders K, Bartholomeus H, Disney MI. 2018. New perspectives on the ecology of tree structure and tree communities through terrestrial laser scanning. *Interface Focus* **8**: 20170052.

Markham J, Fernández Otárola M. 2020. Wind creates crown shyness, asymmetry, and orientation in a tropical montane oak forest. *Biotropica* **52**: 1127–1130.

Meguro S, Miyawaki A. 1994. A study of the relationship between mechanical characteristics and the coastal vegetation among several broad-leaf trees in Miura Peninsula in Japan. *Vegetatio* **112**: 101–111.

Mitchell SJ. 2013. Wind as a natural disturbance agent in forests: a synthesis. *Forestry* **86**: 147–157.

Momberg M, Hedding DW, Luoto M, le Roux PC. 2021. Exposing wind stress as a driver of fine-scale variation in plant communities. *Journal of Ecology* **109**: 2121–2136.

Moore J, Gardiner B, Sellier D. 2018. Tree mechanics and wind loading. In: Geitmann A, Gril J, eds. *Plant biomechanics: from structure to function at multiple scales.* Cham, Switzerland: Springer International Publishing, 79–106.

Moulia B, Combes D. 2004. Thigmomorphogenetic acclimation of plants to moderate winds greatly affects height structure in field-gown alfalfa (*Medicago*

© 2025 The Author(s).
New Phytologist © 2025 New Phytologist Foundation. This article has been contributed to by U.S. Government employees and their work is in the public domain in the USA.

14698137, 0, Downloaded from https://nph.onlinelibrary.wiley.com/doi/10.1111/nph.70294 by Maria Uriarte - Columbia University Libraries , Wiley Online Library on [12/06/2025]. See the Terms and Conditions (https://onlinelibrary.wiley.com/terms-and-conditions) on Wiley Online Library for rules of use; OA articles are governed by the applicable Creative Commons License

sativa L.), an indeterminate herb. *Comparative Biochemistry and Physiology Part A: Molecular & Integrative Physiology* **137**: 8.

Muscarella R, Kolyaie S, Morton DC, Zimmerman JK, Uriarte M. 2020. Effects of topography on tropical forest structure depend on climate context. *Journal of Ecology* **108**: 145–159.

Needham JF, Arellano G, Davies SJ, Fisher RA, Hammer V, Knox RG, Mitre D, Muller-Landau HC, Zuleta D, Koven CD. 2022. Tree crown damage and its effects on forest carbon cycling in a tropical forest. *Global Change Biology* **28**: 5560–5574.

Nicoll BC, Connolly T, Gardiner BA. 2019. Changes in spruce growth and biomass allocation following thinning and guying treatments. *Forests* **10**: 253.

Nicoll BC, Gardiner BA, Peace AJ. 2008. Improvements in anchorage provided by the acclimation of forest trees to wind stress. *Forestry* **81**: 389–398.

Niklas KJ. 1997. Adaptive walks through fitness landscapes for early vascular land plants. *American Journal of Botany* **84**: 16–25.

Niklas KJ. 2016. Tree biomechanics with special reference to tropical trees. In: Goldstein G, Santiago LS, eds. *Tropical tree physiology: adaptations and responses in a changing environment*. Cham, Switzerland: Springer International Publishing, 413–435.

Niklas KJ, Kerchner V. 1984. Mechanical and photosynthetic constraints on the evolution of plant shape. *Paleobiology* **10**: 79–101.

Niklas KJ, Spatz H-C. 2010. Worldwide correlations of mechanical properties and green wood density. *American Journal of Botany* **97**: 1587–1594.

Pan Y, Birdsey RA, Phillips OL, Houghton RA, Fang J, Kauppi PE, Keith H, Kurz WA, Ito A, Lewis SL *et al.* 2024. The enduring world forest carbon sink. *Nature* **631**: 563–569.

Pateiro-Lopez B, Rodriguez-Casal A. 2022. ALPHAHULL: generalization of the convex hull of a sample of points in the plane. [WWW document] URL https://CRAN.R-project.org/package=alphahull.

Peltola HM. 2006. Mechanical stability of trees under static loads. *American Journal of Botany* **93**: 1501–1511.

Peterson CJ. 2019. Damage diversity as a metric of structural complexity after forest wind disturbance. *Forests* **10**: 85.

Quine CP, Gardiner BA. 2007. Understanding how the interaction of wind and trees results in windthrow, stem breakage, and canopy gap formation. In: Johnson EA, Miyanishi K, eds. *Plant disturbance ecology*. Burlington, VT, USA: Academic Press, 103–155.

Quine CP, Gardiner BA, Moore J. 2021. Wind disturbance in forests: the process of wind created gaps, tree overturning, and stem breakage. In: Johnson EA, Miyanishi K, eds. *Plant disturbance ecology, 2nd edn*. San Diego, CA, USA: Academic Press, 117–184.

Quinn PF, Beven KJ, Lamb R. 1995. The in(a/tan/β) index: how to calculate it and how to use it within the topmodel framework. *Hydrological Processes* **9**: 161–182.

R Core Team. 2021. *R: a language and environment for statistical computing*. Vienna, Austria: R Foundation for Statistical Computing.

Ramirez A. 2015. Meteorological data from towers (pre-Hugo) or rooftop (post Hugo) at El Verde. Environmental Data Initiative. [WWW document] URL https://portal.edirepository.org/nis/mapbrowse?packageid=knb-lter-luq.33.471801.

Reilly S, Clark ML, Bentley LP, Matley C, Piazza E, Oliveras Menor I. 2021. The potential of multispectral imagery and 3D point clouds from unoccupied aerial systems (UAS) for monitoring forest structure and the impacts of wildfire in mediterranean-climate forests. *Remote Sensing* **13**: 3810.

Rifai SW, Muñoz JDU, Negrón-Juárez RI, Arévalo FRR, Tello-Espinoza R, Vanderwel MC, Lichstein JW, Chambers JQ, Bohlman SA. 2016. Landscape-scale consequences of differential tree mortality from catastrophic wind disturbance in the Amazon. *Ecological Applications* **26**: 2225–2237.

Ripley B, Venables B, Bates DM, Hornik K, Gebhardt A, Firth D. 2022. MASS: support functions and datasets for venables and Ripley's MASS. [WWW document] URL https://CRAN.R-project.org/package=MASS.

Robertson A. 1986. Estimating mean windflow in hilly terrain from tamarack (*Larix lancina* (Du Roi) K. Koch) deformation. *International Journal of Biometeorology* **30**: 333–349.

Roussel J-R. 2021. lidR: Airborne LiDAR data manipulation and visualization for forestry applications.

Shapiro SS, Wilk MB. 1965. An analysis of variance test for normality (complete samples). *Biometrika* **52**: 591–611.

Smith-Martin CM, Muscarella R, Ankori-Karlinsky R, Delzon S, Farrar SL, Salva-Sauri M, Thompson J, Zimmerman JK, Uriarte M. 2022. Hurricanes increase tropical forest vulnerability to drought. *New Phytologist* **235**: 1005–1017.

Strigul N, Pristinski D, Purves D, Dushoff J, Pacala S. 2008. Scaling from trees to forests: tractable macroscopic equations for forest dynamics. *Ecological Monographs* **78**: 523–545.

Swenson NG, Stegen JC, Davies SJ, Erickson DL, Forero-Montaña J, Hurlbert AH, Kress WJ, Thompson J, Uriarte M, Wright SJ *et al.* 2012. Temporal turnover in the composition of tropical tree communities: functional determinism and phylogenetic stochasticity. *Ecology* **93**: 490–499.

Taylor BN, Stedman E, Van Bloem SJ, Whitmire SL, DeWalt SJ. 2023. Widespread stem snapping but limited mortality caused by a category 5 hurricane on the Caribbean Island of Dominica. *Forest Ecology and Management* **532**: 120833.

Telewski FW. 1995. Wind-induced physiological and developmental responses in trees. In: Grace J, Coutts MP, eds. *Wind and trees*. Cambridge, UK: Cambridge University Press, 237–263.

Thompson J, Brokaw N, Zimmerman JK, Waide RB, Everham EM III, Lodge DJ, Taylor CM, García-Montiel D, Fluet M. 2002. Land use history, environment, and tree composition in a tropical forest. *Ecological Applications* **12**: 1344–1363.

Uriarte M, Canham CD, Thompson J, Zimmerman JK. 2004. A neighborhood analysis of tree growth and survival in a hurricane-driven tropical forest. *Ecological Monographs* **74**: 591–614.

Uriarte M, Clark JS, Zimmerman JK, Comita LS, Forero-Montaña J, Thompson J. 2012. Multidimensional trade-offs in species responses to disturbance: implications for diversity in a subtropical forest. *Ecology* **93**: 191–205.

Uriarte M, Thompson J, Zimmerman JK. 2019. Hurricane María tripled stem breaks and doubled tree mortality relative to other major storms. *Nature Communications* **10**: 1–7.

Van Bloem SJ, Lugo AE, Murphy PG. 2006. Structural response of caribbean dry forests to hurricane winds: a case study from Guánica forest, Puerto Rico. *Journal of Biogeography* **33**: 517–523.

Walker LR. 1991. Tree damage and recovery from hurricane Hugo in Luquillo experimental forest, Puerto Rico. *Biotropica* **23**: 379–385.

Weaver PL. 1991. *Buchenavia capitata (Vahl) Eichl. Granadillo. Combretaceae. Combretum family*. Washington, DC, USA: USDA Forest Service, Southern Forest Experiment Station, Institute of Tropical Forestry, 7.

Yaffar D, Lugo AE, Silver W, Cuevas E, Molina Colon S. 2019. Plant root trait measurements raw data, 1962–2018, Island of Puerto Rico. United States. [WWW document] URL https://www.osti.gov/dataexplorer/biblio/dataset/1558773.

Yaffar D, Norby RJ. 2020. A historical and comparative review of 50 years of root data collection in Puerto Rico. *Biotropica* **98**: 283.

Zhang J, Heartsill-Scalley T, Bras RL. 2022. Parsing long-term tree recruitment, growth, and mortality to identify hurricane effects on structural and compositional change in a tropical forest. *Forests* **13**: 796.

Zimmerman JK, Hogan JA, Shiels AB, Bithorn JE, Carmona SM, Brokaw N. 2014. Seven-year responses of trees to experimental hurricane effects in a tropical rainforest, Puerto Rico. *Forest Ecology and Management* **332**: 64–74.

Zimmerman JK, Wood TE, González G, Ramirez A, Silver WL, Uriarte M, Willig MR, Waide RB, Lugo AE. 2021. Disturbance and resilience in the Luquillo Experimental Forest. *Biological Conservation* **253**: 108891.

Supporting Information

Additional Supporting Information may be found online in the Supporting Information section at the end of the article.

© 2025 The Author(s).
New Phytologist © 2025 New Phytologist Foundation. This article has been contributed to by U.S. Government employees and their work is in the public domain in the USA.

14698137, 0, Downloaded from https://nph.onlinelibrary.wiley.com/doi/10.1111/nph.70294 by Maria Uriarte - Columbia University Libraries , Wiley Online Library on [12/06/2025]. See the Terms and Conditions (https://onlinelibrary.wiley.com/terms-and-conditions) on Wiley Online Library for rules of use; OA articles are governed by the applicable Creative Commons License

Fig. S1 Direction of prevailing winds in the Luquillo Forest Dynamics Plot.

Fig. S2 Distributions of tree height (m), diameter at breast height (cm), crown area (m^2), and crown volume (m^3) of 124 trees in this study.

Fig. S3 Pearson's correlations of environmental variables and architectural metrics of all 124 trees in this study.

Fig. S4 Log–log allometric relationships between stem diameter at breast height (cm) and height*crown area (m^2) of 124 trees in this study.

Notes S1 Derivation of estimated wind vulnerability of individual tree stem break.

Table S1 Results of full multiple linear regression models for height (m) and crown area (m^2) for 124 trees in this study.

Table S2 Results of full multiple linear regression models for slenderness (height/diameter at breast height, m) and estimated wind vulnerability (Eqn 2 in main text; Notes S1) for 124 trees in this study.

Please note: Wiley is not responsible for the content or functionality of any Supporting Information supplied by the authors. Any queries (other than missing material) should be directed to the *New Phytologist* Central Office.

Disclaimer: The New Phytologist Foundation remains neutral with regard to jurisdictional claims in maps and in any institutional affiliations.

New Phytologist © 2025 New Phytologist Foundation. This article has been contributed to by U.S. Government employees and their work is in the public domain in the USA.

© 2025 The Author(s).

14698137, 0, Downloaded from https://nph.onlinelibrary.wiley.com/doi/10.1111/nph.70294 by Maria Uriarte - Columbia University Libraries , Wiley Online Library on [12/06/2025]. See the Terms and Conditions (https://onlinelibrary.wiley.com/terms-and-conditions) on Wiley Online Library for rules of use; OA articles are governed by the applicable Creative Commons License